

Identification of optimal segmentation parameters for extracting buildings from remote sensing images with different resolutions

Aly M. El-Naggar¹, Ramadan Kh. Abdel-maguid¹, Moustafa A. Elsebaei¹, Sami M. Ayaad¹.

Transportation Department, Faculty of Engineering, Alexandria University, Egypt.

E-Mail: moustafa.elsebaei@alexu.edu.eg

ABSTRACT

Remote sensing is now essential across many fields, thanks to advanced techniques and expanding applications. Some objects may share similar geographical conditions but possess varied spectral properties, while others may differ in geographical features but display similar spectral properties. This illustrates that spectral information alone cannot suffice for precise spatial information, thus emphasizing the significance of spatial and contextual information. Measures of homogeneity and heterogeneity frequently assess image criteria, including spectrum, space, texture, shape, size, context, time, and prior knowledge. Therefore, many researchers have shifted their focus toward unconventional methods like Object-Based Image Analysis (OBIA) to extract data from high-resolution images with greater precision. The first step in the OBIA technique is segmentation, which involves dividing an image into relatively homogeneous areas or segments. Selecting appropriate segmentation parameters compactness, shape, and scale is a fundamental stage in the image segmentation process. There is currently a shortage of global models or frameworks for computing scale parameters, as well as a lack of universal methods or algorithms in this area. It is important to note that there is no one-size-fits-all scale for image objects with varying sizes, shapes, and spatial distributions that are present in a scene.

The main objective of this research is to identify the optimal values for the parameters used in image segmentation. Therefore, this research has utilized Worldview-3, Worldview-2, and GeoEye-1 images with varying parameter values to understand the relationship between parameters and image resolution by keeping most variables fixed and using different-resolution images of the same area.

Keywords segmentation parameter, Multiresolution segmentation, Segmentation.

1. Introduction

Over the past decade, satellite systems have advanced to the point where they can observe objects at a spatial resolution of less than 1 meter. This has resulted in the observed object dimension being significantly larger than the size of each pixel. As a result, the conventional pixel-based method is unsuitable for analyzing images of high spatial resolution, which contain a large amount of detail. Instead, experts have started focusing on the representation of groups of pixels, known as objects, as the most appropriate input data for analysis. This process of identifying and distinguishing between different geographical objects is enabled by using the OBIA.

The OBIA method has become increasingly popular as a means of combining the segmentation and classification of remote-sensing images. This method involves dividing the image into parts containing homogeneous pixels, which are then categorized to achieve the classification purpose. The goal of classification is to determine the names and characteristics of these groups on the earth's surface. The operator selects groups of similar pixels in visual interpretation to identify land use classes.

The initial stage of object-based classification involves collecting pixels with consistent fundamental characteristics. Then, based on various attributes, these segments are accurately classified. By utilizing the OBIA method, the benefits of pixel-

based and optical classification are combined[1].

The Object-based Image Analysis (OBIA) technique is widely used in building studies because it can group pixels in an image into homogeneous objects using an image segmentation algorithm, and then classify each object[2]. This method has become one of the most commonly used remote sensing techniques[3]. Moreover, the OBIA method is currently quite significant in image classification, as it takes into account shape, texture, and spectral data[4]. However, the accuracy of the classification process using the OBIA method depends on segmentation, feature selection, and classifier determination. According to [3], the quality of the image classification method depends mainly on the quality of the segmentation process, which in turn depends on a large number of parameter values for segmentation. In the field of image segmentation, two types of segmentation errors are over-segmentation and under-segmentation. Over-segmentation occurs when a portion of the image is divided into smaller segments than the object it represents. Conversely, under-segmentation occurs when the segmented regions are larger than the actual object. In the case of over-segmentation, it is possible to miss the object, while in the case of under-segmentation, it can be difficult to accurately identify the object. Therefore, it is important to choose the best segmentation parameters to avoid under-segmentation errors.

2 Identification of optimal segmentation parameters for extracting buildings from remote sensing images

2. Study Area

The study area for this research is located in the West of Tabaco City, Philippines. It covers an approximate area of 484,014m² and includes a variety of urban land uses such as high-density residential areas, road networks, and different proportions of grass and tree-covered zones. The area was selected because it meets the required degree of variability and heterogeneity.

3. Data Used

In this research, the initial step involved using an orthorectified Worldview-3 multispectral satellite image to determine the optimal segmentation parameters for extracting buildings from satellite images. The image has a spatial resolution of 36 cm and is shown in Fig (1).

The second image in this research is an orthorectified GeoEye-1 multispectral satellite image that was utilized to determine the best segmentation parameters that can be used to extract buildings from satellite images Fig (2). the resolution of the image is 45 cm.

The third image in this research is an orthorectified Worldview-2 multispectral satellite image that was utilized to determine the best segmentation parameters that can be used to extract Buildings from satellite images Fig (3). the spatial resolution of the image is 58 cm.

Table (1) shows the most important characteristics of the multispectral images that were used in this r research.



Fig. (1) Worldview-3 multispectral image.



Fig. (2) GeoEye-1 multispectral image.



Fig. (3) WorldView-2 multispectral image.

Table (1) Characteristics of the multispectral images

Image	WorldView-3	GeoEye-1	WorldView-2
Image Type	Ortho Ready Standard	Ortho Ready Standard	Ortho Ready Standard
Acquisition Date	23 Sep 2020	23 July 2020	9 July 2020
Cloud Cover	Cloud-free	Cloud-free	Cloud-free
bits per pixel	16 bits per pixel	16 bits per pixel	16 bits per pixel
Multispectral bands	Blue (20-215)	Blue (13-221)	Blue (41-198)
	Green (29-232)	Green (27-235)	Green (61-214)
	Red (233-240)	Red (10-239)	Red (43-217)
Spatial resolution	0.36 m	0.45 m	0.58 m
projection	UTM_Zone_51	UTM_Zone_51	UTM_Zone_51
Datum	WGS_1984	WGS_1984	WGS_1984
Dimensions	2390 x 1652 Pixel	1750 x 1349 Pixel	1339 x 1067 Pixel
	779.70x 620.77m	779.98x 621.31m	779.45 x 621.1m

4. Methodology

The study was conducted in four phases as shown in Fig (4), with the initial phase consisting of data acquisition from Open Aerial Map (OAM)[5], The three images were rectified and resampled using cubic convolution method. During the second phase, an OBIA (Object-Based Image Analysis) technique was utilized. This technique involves image segmentation, feature selection, and image classification. Multiresolution segmentation was performed using eCognition software, and the relevant parameters such as scale, shape, and compactness were optimized to select the most significant value. In the third phase, the evaluation process was utilized by selecting evaluation samples and using evaluation matrices. Finally, data were analyzed, and the optimum parameters for each image were determined.

4.1. Object-based image analysis

In this paper, we performed a series of segmentations using the three images with different segmentation parameter values. Our goal was to identify the ideal or nearly ideal segmentation parameter values for scale, shape, and compactness, based on the combination of values presented in table (2). To accomplish this,

we used the multiresolution segmentation algorithm (MRS) within the eCognition software, employing an object-based image analysis (OBIA) approach. The eCognition software was developed by Definiens for analyzing and segmenting remote-sensing images[6]. A total of 1008 trials occur across the three images, with 336 trials in each image.

Figure (5) presents the segmentation outcomes in the WorldView-3 image, using the following parameter values: 25, 0.10, and 0.70 for the scale, shape, and compactness parameters, respectively. The boundary lines of each segment are shown in blue in the image.

Figure (6) displays the results of image segmentation using scale, shape, and compactness parameters of 50, 0.60, and 0.70 respectively on a GeoEye-1 image.

Figure (7) displays the results of image segmentation using scale, shape, and compactness parameters of 150, 0.80, and 0.60 respectively on a WorldView-2 image.

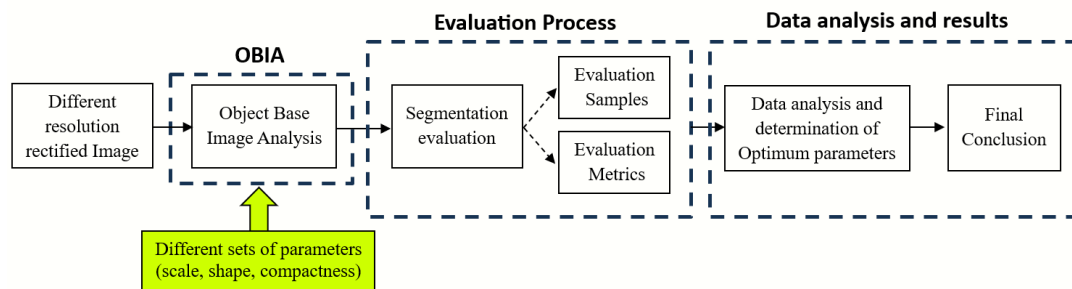


Fig. (4) Research methodology flowchart.

Table (2) The value of used segmentation parameters

Scale	25	50	75	100	125	150		
Shape	0.1	0.2	0.3	0.4	0.5	0.6	0.7	0.8
Compactness	0.3	0.4	0.5	0.6	0.7	0.8	0.9	

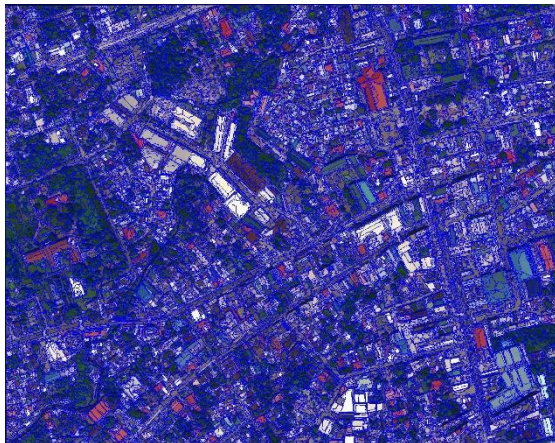


Fig. (5) WorldView-3 Segmentation results for Scale = 25, Shape = 0.10, and Compactness = 0.70.

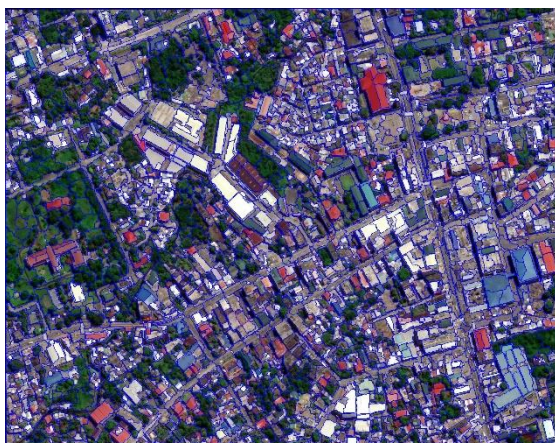


Fig. (6) GeoEye-1 Segmentation results for Scale = 50, Shape = 0.60, and Compactness = 0.70.



Fig. (7) WorldView-2 Segmentation results for Scale = 150, Shape = 0.80, and Compactness = 0.60.

4.2. Segmentation evaluation

Segmentation assessment techniques can be broadly classified into two categories: supervised and unsupervised. In supervised approaches, it is necessary to adjust the segmentation parameters using reference data to achieve a situation where the image objects match the ground reference object. Supervised methods are preferable for assessing segmentation results, particularly when precise ground reference data is available[7].

A set of metrics is employed to assess the accuracy of image segmentation. These metrics involve matching the segmented object with the reference object and evaluating the interaction between the area value of the segmented object and the reference object. This process helps in determining the quality of the segmentation process.

Table (3) displays various methods used to evaluate the segmentation of remote sensing images, along with their corresponding mathematical models.

Table (3) Overview of the segmentation accuracy metrics

Segmentation Accuracy Metric	Mathematical Formula
Quality rate	$QR = 1 - \frac{A_{Rj} \cap A_{Si}}{A_{Ri} \cup A_{Si}}$
Area fit index	$AFI = 1 - \frac{A_{Rj} - A_{Si}}{A_{Ri}}$
Over segmentation	$OS = 1 - \frac{A_{Rj} \cap A_{Si}}{A_{Ri}}$
Under segmentation	$QR = 1 - \frac{A_{Rj} \cap A_{Si}}{A_{Si}}$
Root mean square	$D = \sqrt{\frac{(OS)^2 + (US)^2}{2}}$

where A_{Rj} refers to the reference total area R_j , and A_{Si} refers to the total area of corresponding terrain segments [8].

The area fit index (AFI), quality rate (QR), and root mean square (D) are metrics that are used to assess the overall quality of an image segmentation. The D metric combines the over-segmentation (OS) and under-segmentation (US) metrics to evaluate the degree of similarity between the image objects and the reference objects. The use of US and OS metrics is known as local effectiveness because it takes into account the individual objects in the image.

Over-segmentation occurs when adjacent parts lack enough contrast and need to be combined into one object. On the other hand, under-segmentation happens when there are areas within the image that are larger than the object they belong to and need to be divided into smaller parts[7].

The metrics used in image segmentation have a value ranging between zero and one. This value indicates how close the segmentation results are to the actual ground reference object. The closer the value is to zero, the more accurate the segmentation

process is. However, in cases where there is under-segmentation, the value will be less than zero[8].

To accurately evaluate the segmentation results of each group, we analyzed eleven reference buildings that varied in location, shape, size, texture, contrast, and other pertinent factors and they are numbered in descending order according to their area.

We then compared visually and geometrically simulated versions of each building with the segmented regions, as seen in Figure (8).

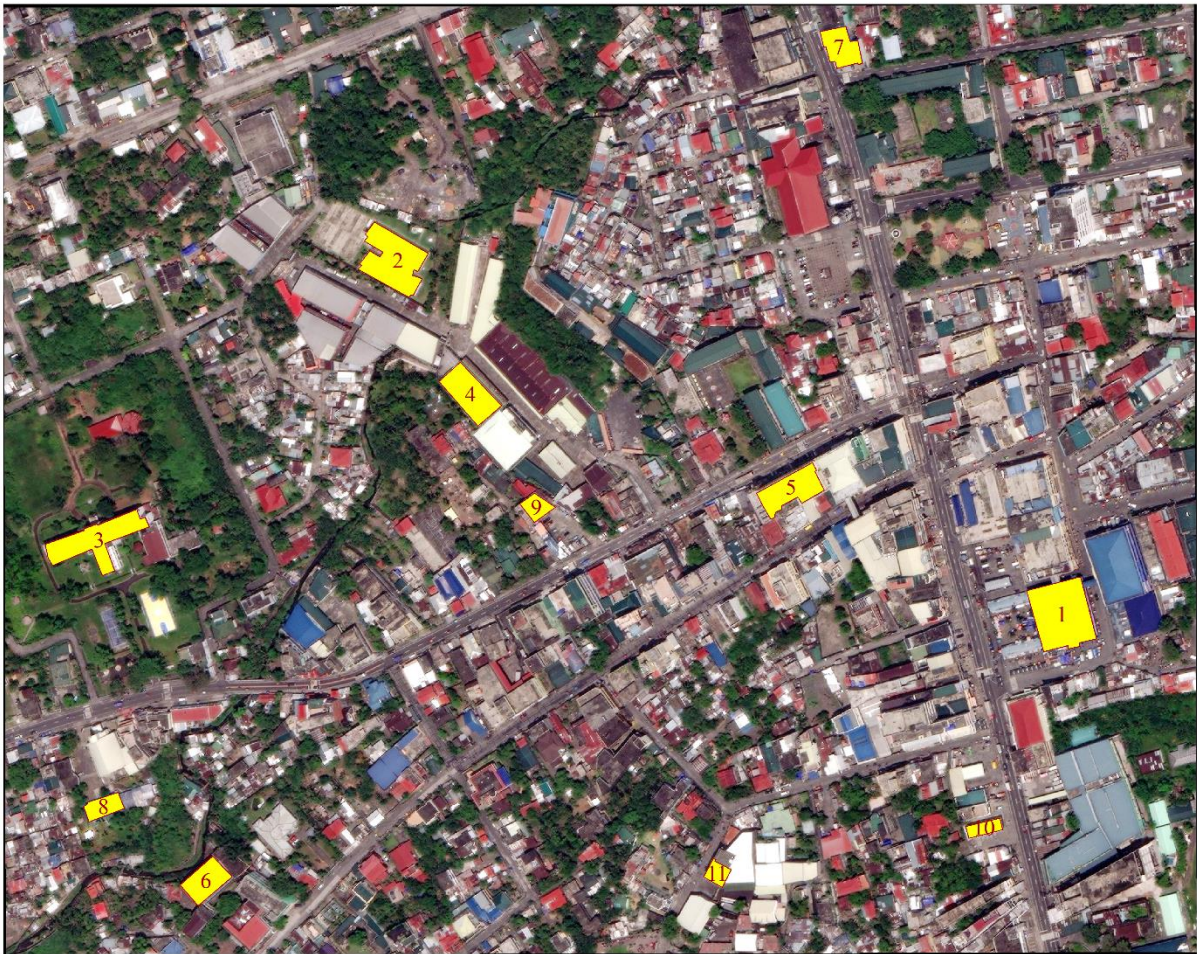


Fig (8) Eleven buildings were used to assess the accuracy of classification.

5. Experimental analysis and discussion

In this paper, a set of segmentations was carried out utilizing the three images shown above with different values for the segmentation parameters to define ideal or close ideal segmentation parameters (scale, shape, and compactness) values according to the combination values shown in table (2). In this study, there were many attempts, which reached 336 sets for each image of the three parameters scale = (25, 50, 75, 100, 125, 150), shape = (0.10, 0.20, 0.30, 0.40, 0.50, 0.60, 0.70, 0.80) and compactness = (0.30, 0.40, 0.50, 0.60, 0.70, 0.80) were utilized for the segmentation of the three images.

Since the human eye is an experienced tool for

evaluating segmentation methods[1], some trials are evaluated visually, such as the results presented in figure (5) and figure (7). As is clear in figure (5) the process is over-segmentation while figure (7) is under-segmentation.

In figure (6), many segments appear satisfactory; hence, it was evaluated using table (4). The first column indicates the building number, while the second column represents the actual reference area of each building. The third column shows the area of the largest part that was segmented and shares the reference area in a portion of the area. The fourth to eighth columns represent different goodness metrics that were previously

shown in Table (3).

Based on our analysis of the data and results, we have noted a marked contrast in the performance of the buildings. Specifically, buildings numbered 1-5, which boast larger areas, outperformed those numbered 6-11 with smaller areas. As a result, it is

not feasible to utilize a single set of optimal parameters that would be effective for all buildings. Rather, we have categorized the parameters into two groups: one for homogeneous buildings and the other for heterogeneous buildings.

Table (4) Shows the segmentation evaluation for each building for segmentation parameters Scale=50, Shape =0.6 and compactness = 0.7 for GeoEye-1 multispectral image

Building	Ar	As	Quality Rate (QR)	Area Fit Index (AFI)	Oversegmentation (OS)	Undersegmentation (US)	Root Mean Square (D)
1	1512.60				Over-segmentation		
2	1211.22				Over-segmentation		
3	1072.94				Over-segmentation		
4	756.44	713.75	0.068	0.06	0.06	0.006	0.044
5	725.81				Over-segmentation		
6	522.37	543.5	0.074	-0.04	0.02	0.057	0.042
7	479.44	542.31	0.119	-0.13	0.002	0.118	0.083
8	286.93	328.37	0.197	-0.14	0.045	0.165	0.121
9	222.56	305.52	0.320	-0.37	0.040	0.300	0.214
10	180.53	159.91	0.144	0.11	0.130	0.018	0.093
11	178.76	169.95	0.128	0.05	0.092	0.045	0.072

Table (5) presents the evaluation of optimum segmentation parameters for WorldView-3, with Scale=50, Shape=0.6, and Compactness=0.6, for small-area buildings. The best results for such buildings are shown in figure (9) presents the best results.

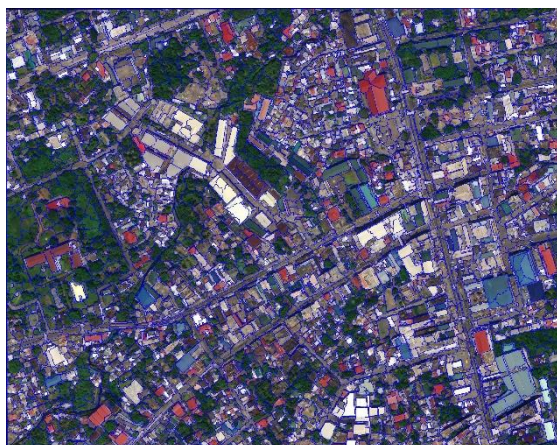


Fig. (9) WorldView-3 optimum Segmentation parameters Scale =50, Shape = 0.60, and Compactness = 0.60.

Table (6) presents the evaluation of optimum segmentation parameters for WorldView-3, with Scale=150, Shape=0.4, and Compactness=0.6, for Large-area buildings. The best results for such buildings are shown in figure (10) presents the best results.

Table (7) presents the evaluation of optimum segmentation parameters for GeoEye-1, with Scale=50, Shape=0.6, and Compactness=0.8, for

Small-area buildings. Figure (11) displays the best results.

Table (8) presents the evaluation of optimum segmentation parameters for GeoEye-1, with Scale=150, Shape=0.2, and Compactness=0.9, for large-area buildings. Figure (12) displays the best results.



Fig. (10) WorldView-3 optimum Segmentation parameters Scale = 150, Shape = 0.40, and Compactness = 0.60.

Table (9) shows the optimal segmentation parameters for small-area buildings using WorldView-2, with Scale=50, Shape=0.6, and Compactness=0.5. Figure (13) illustrates the best results.

Table (10) shows the optimal segmentation parameters for large-area buildings using WorldView-2, with Scale=125, Shape=0.3, and Compactness=0.2. Figure (14) illustrates the best results.

Table (5) Shows the segmentation evaluation for each building for segmentation parameters Scale=50, Shape =0.6 and compactness = 0.6 for WorldView-3 multispectral image small-area buildings

Building	Ar	As	Quality Rate (QR)	Area Fit Index (AFI)	Oversegmentation (OS)	Undersegmentation (US)	Root Mean Square (D)
1	1512.60				Over-segmentation		
2	1211.22				Over-segmentation		
3	1072.94				Over-segmentation		
4	756.44	707.27	0.093	0.065	0.080	0.016	0.058
5	725.81				Over-segmentation		
6	522.37	508.9	0.090	0.026	0.060	0.035	0.049
7	479.44	484.85	0.066	-0.011	0.029	0.040	0.035
8	286.93	300.16	0.126	-0.046	0.045	0.088	0.070
9	222.56	227.48	0.046	-0.022	0.013	0.034	0.026
10	180.53	167.15	0.082	0.074	0.078	0.005	0.056
11	178.76	187.08	-0.047	0.020	0.064	0.047	0.047

Table (6) Shows the segmentation evaluation for each building for segmentation parameters Scale=150, Shape =0.4 and compactness = 0.6 for WorldView-3 multispectral image large-area buildings

Building	Ar	As	Quality Rate (QR)	Area Fit Index (AFI)	Oversegmentation n (OS)	Undersegmentation on (US)	Root Mean Square (D)
1	1512.60	1481.65	0.076	0.020	0.050	0.030	0.041
2	1211.22	1219.5	0.055	0.007	0.025	0.032	0.029
3	1072.94	1021.25	0.119	0.048	0.086	0.040	0.067
4	756.44	760.42	0.037	0.005	0.016	0.021	0.019
5	725.81	731.46	0.039	0.008	0.016	0.024	0.020
6	522.37	625.42	0.168	-0.197	0.002	0.167	0.118
7	479.44	445.12	0.128	0.072	0.102	0.033	0.076
8	286.93	341.35	0.201	-0.190	0.027	0.182	0.130
9	222.56	226.55	0.047	-0.018	0.015	0.033	0.026
10	180.53	239.97	0.248	-0.329	0.001	0.248	0.175
11	178.76	210.34	0.178	-0.177	0.018	0.165	0.118



Fig. (11) GeoEye-1 optimum Segmentation parameters Scale = 50, Shape = 0.60, and Compactness = 0.80.



Fig. (12) GeoEye-1 optimum Segmentation parameters Scale = 150, Shape = 0.20, and Compactness = 0.90.

Table (7) Shows the segmentation evaluation for each building for segmentation parameters Scale=50, Shape =0.6 and compactness = 0.8 for GeoEye-1 multispectral image small-area buildings

Building	Ar	As	Quality Rate (QR)	Area Fit Index (AFI)	Oversegmentation (OS)	Undersegmentation (US)	Root Mean Square (D)
1	1512.60				Over-segmentation		
2	1211.22				Over-segmentation		
3	1072.94				Over-segmentation		
4	756.44	719.51	0.061	0.05	0.06	0.007	0.039
5	725.81				Over-segmentation		
6	522.37	562.77	0.10	-0.08	0.02	0.09	0.06
7	479.44	548.07	0.13	-0.14	0.00	0.13	0.09
8	286.93	299.96	0.17	-0.05	0.07	0.11	0.09
9	222.56	227.85	0.12	-0.02	0.05	0.07	0.06
10	180.53	176.2	0.12	0.02	0.07	0.05	0.06
11	178.76	170.84	0.18	0.04	0.12	0.08	0.10

Table (8) Shows the segmentation evaluation for each building for segmentation parameters Scale=.150 Shape =0.2 and compactness = 0.9 for GeoEye-1 multispectral image large-area buildings

Building	Ar	As	Quality Rate (QR)	Area Fit Index (AFI)	Oversegmentation (OS)	Undersegmentation (US)	Root Mean Square (D)
1	1512.60	1532.38	0.110	-0.013	0.052	0.064	0.058
2	1211.22	1212.75	0.071	-0.001	0.036	0.037	0.037
3	1072.94	1115.41	0.162	-0.040	0.070	0.106	0.090
4	756.44	759.44	0.093	-0.004	0.047	0.051	0.049
5	725.81	688.72	0.081	0.051	0.067	0.016	0.048
6	522.37	640.05	0.190	-0.225	0.004	0.187	0.133
7	479.44	482.32	0.113	-0.006	0.057	0.062	0.060
8	286.93	259.24	0.159	0.097	0.131	0.038	0.096
9	222.56	1543.7	0.863	-5.936	0.043	0.862	0.610
10	180.53	168.45	0.131	0.067	0.101	0.037	0.076
11	178.76	1510.72	0.894	-7.451	0.093	0.893	0.635

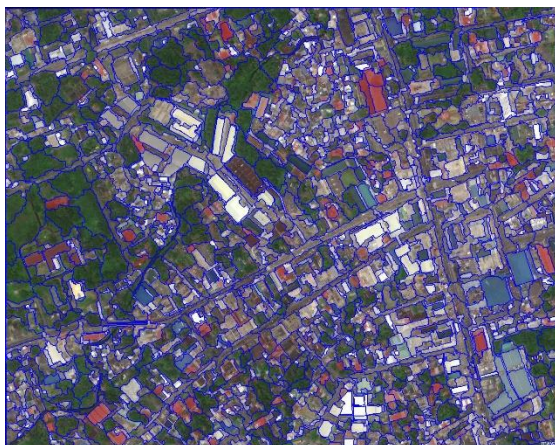


Fig. (13) WorldView-2 optimum Segmentation parameters Scale = 50, Shape = 0.60, and Compactness = 0.50.



Fig. (14) WorldView-2 optimum Segmentation parameters Scale = 125, Shape = 0.30, and Compactness = 0.20.

Table (9) Shows the segmentation evaluation for each building for segmentation parameters Scale=50, Shape =0.6 and compactness = 0.5 for WorldView-2 multispectral image small-area buildings

Building	Ar	As	Quality Rate (QR)	Area Fit Index (AFI)	Oversegmentation (OS)	Undersegmentation (US)	Root Mean Square (D)
1	1512.60				Over-segmentation		
2	1211.22				Over-segmentation		
3	1072.94				Over-segmentation		
4	756.44	725.13	0.118	0.041	0.082	0.042	0.065
5	725.81	682.78	0.168	0.059	0.119	0.063	0.095
6	522.37	584.51	0.130	-0.119	0.014	0.119	0.085
7	479.44	471.34	0.079	0.017	0.049	0.033	0.042
8	286.93	245.66	0.229	0.144	0.192	0.056	0.142
9	222.56	218.89	0.073	0.016	0.046	0.030	0.039
10	180.53	187.04	0.110	-0.036	0.041	0.075	0.060
11	178.76	201.28	0.126	-0.126	0.008	0.119	0.085

Table (10) Shows the segmentation evaluation for each building for segmentation parameters Scale=125, Shape =0.3 and compactness = 0.2 for WorldView-2 multispectral image large-area buildings

Building	Ar	As	Quality Rate (QR)	Area Fit Index (AFI)	Oversegmentation (OS)	Undersegmentation (US)	Root Mean Square (D)
1	1512.60	1415.71	0.092	0.064	0.079	0.016	0.057
2	1211.22	1207.65	0.073	0.003	0.039	0.036	0.038
3	1072.94	1133.78	0.150	-0.057	0.055	0.106	0.084
4	756.44	722.76	0.082	0.045	0.064	0.021	0.048
5	725.81	693.28	0.142	0.045	0.097	0.055	0.079
6	522.37	615.69	0.165	-0.179	0.009	0.159	0.113
7	479.44	678.71	0.359	-0.416	0.057	0.334	0.239
8	286.93	2280.1	0.879	-6.947	0.034	0.878	0.622
9	222.56	1392.66	0.847	-5.257	0.037	0.846	0.599
10	180.53	231.77	0.221	-0.284	0.000	0.221	0.156
11	178.76	233.8	0.258	-0.308	0.017	0.249	0.176

It was observed that optimal parameters for extracting buildings from an image vary for large and small areas, hence there are no fixed parameters for all areas.

It has been observed that Building No. 3 and Building No. 4 have similar areas, but Building No. 4 produces better results in most cases. The reason behind this is that Building No. 4 has a regular shape, while Building No. 3 has an irregular shape and borders. Hence, there is a difference between homogeneous and heterogeneous shapes.

6. Conclusion

After conducting image segmentation on the remote sensing image of the case study, using different resolution images of the same area while keeping most variables fixed led to a set of conclusions.

1. It's important to note that there is no one set of parameters that fits all image objects with varying sizes, shapes, and spatial distributions present in a scene.

2. pre-estimation of parameters that provide reliable results, balancing between intersegment heterogeneity measures and intersegment homogeneity measures, using adaptive scaling.

3. The MRS segmentation algorithm in eCognition considers only scale, shape, and compactness for segmentation, but future works could include additional parameters such as texture, and intensity.

4. Table (11) shows how OBIA researchers can target specific parameter values based on different resolution images and building sizes.

Table (11) The optimum segmentation parameters for all cases of study

Parameters	WorldView-3		GeoEye-1		WorldView-3	
	Small Area	Large Area	Small Area	Large Area	Small Area	Large Area
Scale	50	150	50	150	50	125
Shape	0.6	0.4	0.6	0.2	0.6	0.3
Compactness	0.6	0.6	0.8	0.9	0.5	0.2

References

- [1] T. Veljanovski, U. Kanjir, and K. J. G. v. Ostir, "Object-based image analysis of remote sensing data," vol. 55, no. 4, pp. 678-688, 2011.
- [2] D. Liu and F. J. R. s. l. Xia, "Assessing object-based classification: advantages and limitations," vol. 1, no. 4, pp. 187-194, 2010.
- [3] A. M. J. A. e. j. El-naggar, "Determination of optimum segmentation parameter values for extracting building from remote sensing images," vol. 57, no. 4, pp. 3089-3097, 2018.
- [4] H. I. Sibaruddin, H. Z. M. Shafri, B. Pradhan, and N. A. J. J. G. G. Haron, "UAV-based approach to extract topographic and as-built information by utilising the OBIA technique," vol. 6, pp. 103-123, 2018.
- [5] OpenAerialMap. (2020, 14April2024). Available: <https://openaerialmap.org/>
- [6] U. C. Benz, P. Hofmann, G. Willhauck, I. Lingenfelder, M. J. I. J. o. p. Heynen, and r. sensing, "Multi-resolution, object-oriented fuzzy analysis of remote sensing data for GIS-ready information," vol. 58, no. 3-4, pp. 239-258, 2004.
- [7] M. Belgiu, L. J. I. J. o. P. Drăguț, and R. Sensing, "Comparing supervised and unsupervised multiresolution segmentation approaches for extracting buildings from very high resolution imagery," vol. 96, pp. 67-75, 2014.
- [8] C. Eisank, M. Smith, and J. J. G. Hillier, "Assessment of multiresolution segmentation for delimiting drumlins in digital elevation models," vol. 214, pp. 452-464, 2014.